European Journal of Chemistry

View Journal Online
View Article Online

A new hydrazide functionalized Schiff's base derivative: Insights into crystallography, Hirshfeld surface, and energy framework analysis

Vivek Prakash Malviya [1] and Archisman Dutta [1,2,*]

[1] *Geological Survey of India, Northern Region, Lucknow-226024, India*
[2] *Department of Chemistry, Institute of Science, Banaras Hindu University, Varanasi-221005, India*

* *Corresponding author at: Geological Survey of India, Northern Region, Lucknow-226024, India.*
e-mail: archisman.dutta@gsi.gov.in (A. Dutta).

RESEARCH ARTICLE

10.5155/eurjchem.13.3.351-357.2310

Received: 18 July 2022
Received in revised form: 04 August 2022
Accepted: 20 August 2022
Published online: 30 September 2022
Printed: 30 September 2022

KEYWORDS

Schiff's base
Crystal structure
Hydrogen bonding
Energy frameworks
Non-covalent interaction
Hirshfeld surface analysis

ABSTRACT

A new hydrazide functionalized Schiff's base derivative, *N'*-(3,4-dichlorobenzylidene)-4-hydroxybenzohydrazide (**I**), has been synthesized using a solvent-assisted mechano-chemical grinding strategy and structurally characterized using elemental analysis, ^{1}H NMR and crystallographic studies. The single crystal X-ray diffraction study depicts that molecule is puckered with two aromatic rings lying out-of-plane in near *anti*-configuration across the C=N bond. The weak interactions involved in supramolecular framework formation are Cl···O, Cl···Cl, Cl···H, Cl···N, C···H, and O···H contacts. The intermolecular O···H interaction being stronger than other dispersive interactions such as halogen bonding, interlocks the molecules in a 2D sheet-type packing. All the structure directing interactions involved in developing crystal architecture are addressed with Hirshfeld surface analysis and fingerprint plots. The energy framework analysis shows visualization of 3D topology of short contacts related to molecular packing of compound **I** which further clarifies the predominance of both Coulombic and dispersive energies in developing supramolecular architecture.

Cite this: *Eur. J. Chem.* **2022**, *13(3)*, 351-357 **Journal website**: www.eurjchem.com

1. Introduction

The rational design of a molecular crystal with a specific desired internal structure, which in turn leads ideally to a specific targeted trait, is known as crystal engineering [1-5]. This target is achieved through self-assembly of molecular subunits, called supramolecular synthons, through non-covalent interactions. Desiraju *et al.* coined the building blocks of supramolecular synthesis as *supramolecular synthons*, an entity that is very similar to *covalent synthons* in retrosynthesis, as put forward by Corey *et al.* [6-8]. Reddy and coworkers advanced this idea to a greater extent by adding the context of supramolecular shape synthons, which focus on shape complementarity along with isotropic/anisotropic weak contacts for the rational design of mechanically flexible molecular single crystals [5]. Noncovalent interactions like hydrogen bonding, π···π interaction, σ-hole interactions like chalcogen bonding, halogen bonding, spodium bonding, *etc.* play a decisive role in the molecular packing inside the crystal lattice to develop the crystal framework [4-13]. For a feasible weak interaction to happen, the strength of an interaction should be above *k*T in energy (*k* = Boltzmann constant) whose value is 0.6 kcal/mol at room temperature. Intermolecular interactions bear energy in the range of 1 to 15 kcal/mol; however, the value increases with an increase in the electrostatic nature of the non-covalent interaction, resulting in a rise of quasi-covalent nature of a non-covalent interaction [1,6]. Another significant aspect for supramolecular crystal architecture formation is directionality of involved weak interactions. Desiraju *et al.* pointed out that the most important directional interaction in molecular crystals is hydrogen bonding whose anisotropic property helps in designing molecular crystals with pre-desired packing and properties [1,6-16]. Therefore, the holistic approach to the study of such weak interactions is very essential to understand the structure-mechanical property relationship of organic molecular crystals [15,16].

Hydrazides are very interesting molecules both in the context of crystal engineering and biologically activity where they are used as drugs for treatment of depression, convulsions, microbial activities, *etc.* [17,18]. The presence of hydrogen bond donor and acceptor sites of hydrazide molecules play crucial roles in the context of crystal engineering. Dutta *et al.* has pointed that due to the strong reactivity of free amine functionality, direct drug application of hydrazides is avoided and hence, hydrazides are initially converted into hydrazones or Schiff's bases and then used for biological activities [9]. Keeping in mind the crystallographic benefices of hydrazides, we report here a new Schiff's base complex, *N'*-(3,4-dichloro-

ISSN 2153-2249 (Print) / ISSN 2153-2257 (Online)
https://dx.doi.org/10.5155/eurjchem.13.3.351-357.2310

Table 1. Crystal data and structure refinement for compound **I**.

Empirical formula	$C_{14}H_{10}Cl_2N_2O_2$
Formula weight	309.14
Temperature (K)	100.00(10)
Crystal system	Orthorhombic
Space group	$P2_12_12_1$
a, (Å)	7.0723(3)
b, (Å)	11.9260(5)
c, (Å)	15.0528(6)
Volume (Å^3)	1269.62(9)
Z	4
ρ_{calc} (g/cm^3)	1.617
μ (mm^{-1})	0.513
F(000)	632.0
Crystal size (mm^3)	0.42 × 0.3 × 0.1
Radiation	MoKα (λ = 0.71073)
2Θ range for data collection (°)	4.36 to 52.64
Index ranges	$-8 \le h \le 6$, $-9 \le k \le 14$, $-18 \le l \le 14$
Reflections collected	2882
Independent reflections	2254 [R_{int} = 0.0200, R_{sigma} = 0.0444]
Data/restraints/parameters	2254/0/182
Goodness-of-fit on F^2	1.039
Final R indexes [I≥2σ (I)]	R_1 = 0.0347, wR_2 = 0.0797
Final R indexes [all data]	R_1 = 0.0378, wR_2 = 0.0831
Largest diff. peak/hole (e.Å^{-3})	0.30/-0.28
Flack parameter	0.03(8)

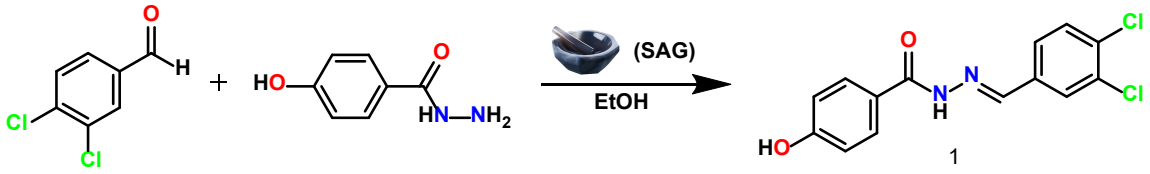

Scheme 1. Synthetic procedure of the Schiff's base **I**.

benzylidene)-4-hydroxybenzohydrazide (**I**), formed by reacting 4-hydroxybenzhydrazide with 3,4-dichlorobenzaldehyde in ethanol solvent using solvent assisted grinding methodology and have characterized the compound with elemental analysis, ^{1}H NMR and single crystal X-ray diffraction studies. The presence of all weak interactions is validated through Hirshfeld surface analysis and fingerprint plots. Energy framework landscape studies provide insight about the nature of the interaction energies involved in stabilizing the crystal framework.

2. Experimental

2.1. Materials and instrumentation

All chemicals are obtained from Sigma-Aldrich and Merck and are of analytical quality. Chemicals are utilized without additional purification, and the solvents employed in the reactions are of reagent grade. The Perkin-Elmer 240 C, H, and N analyzer is used for elemental analysis. In DMSO-d_6 solvent, the ^{1}H NMR spectrum is recorded on a JEOL JNM-ECZ500R/S1 FT NMR (500 MHz) (Japan) spectrophotometer at room temperature, and the chemical shifts observed are quantified in parts per million (δ/ppm) with respect to the internal standard tetramethylsilane (TMS).

2.2. Synthesis and crystallization

3,4-Dichlorobenzaldehyde (1 mmol) and 4-hydroxybenzhydrazide (1 mmol) are grinded slowly in a mortar and pestle using solvent (ethanol) assisted mechanochemical grinding methodology (SAG) for nearly 10-15 minutes, until the compounds are homogeneously mixed as recently reported by Dutta *et al.* [9]. The mixture is then transferred to a 100 mL conical flask and 20-30 mL of ethanol solvent is added to it followed by slow heating on a hot mantle at 60-70 °C for 30 minutes. The resultant supernatant solution is filtered hot and kept for crystallization by covering the conical flask with aluminium foil. The slow evaporation of the solvent furnished plate-shaped colorless crystals of Schiff's base **I** which are suitable for single crystal X-ray diffraction experiment after five days (Scheme 1).

N'-(3,4-Dichlorobenzylidene)-4-hydroxybenzohydrazide (**I**): Color: Colorless. M.p.: 154 °C. Yield: 0.212 g (~90%). ^{1}H NMR (500 MHz, DMSO-d_6, δ, ppm): 8.54 (s, 1H), 8.26 (s, 1H), 8.00 (s, 1H), 7.67 (d, 2H, *J* = 8 Hz), 7.86 (d, 1H, *J* = 8 Hz), 7.88 (d, 1H, *J* = 8 Hz), 6.88 (d, 2H, *J* = 8 Hz), 5.35 (s, 1H). Anal. calcd. for $C_{14}H_{10}Cl_2N_2O_2$: C, 54.39; H, 3.26; N, 9.06. Found: C, 55.03; H, 3.74; N, 9.76 %.

2.3. Single crystal X-ray diffraction (SCXRD)

The graphite monochromated Mo-Kα radiation (λ = 0.71073 Å) is used in single crystal X-ray diffraction studies at 100 K utilising an ω-scan technique in a SuperNova (Dual, Cu at zero, Eos) instrument equipped with a four-circle diffractometer with experimental absorption process CrysAlisPro 1.171.38.41 and empirical absorption correction using spherical harmonics, implemented in the SCALE3 ABSPACK scaling algorithm [19]. The structure is solved using SHELXT 2018/2 and refined with SHELXL enabled with the least squares model in Olex2 1.3-alpha software [20,21]. All non-hydrogen atoms are refined anisotropically and all hydrogen atoms are generated geometrically and refined isotropically [22,23] (Figure 1 and Table 1).

2.4. Hirshfeld surface and energy framework analysis

CrystalExplorer 21.2 is used to construct Hirshfeld surfaces, 2D fingerprint plots, and energy framework calculations [24]. Hirshfeld surfaces are mapped with distinct surface characteristics, including d_{norm}, d_e, d_i, shape index, surface curvedness,

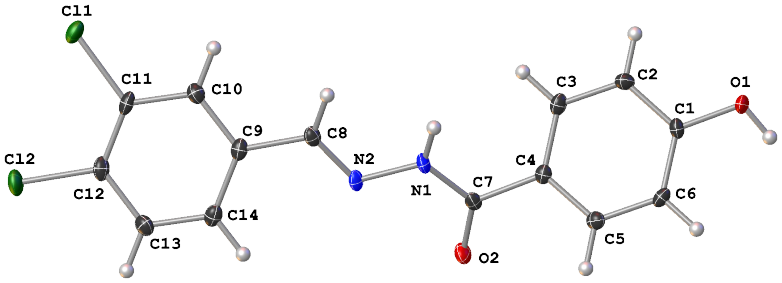

Figure 1. ORTEP diagram of Schiff base **I** at the 50% ellipsoid probability level.

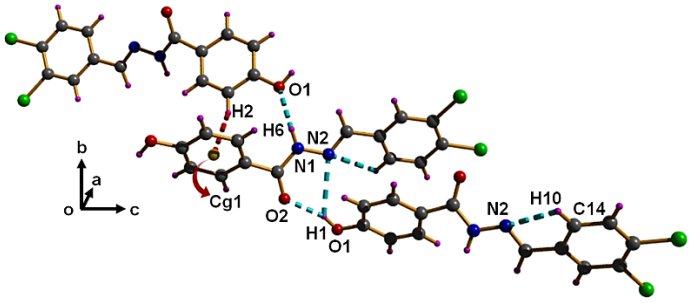

Figure 2. Diagram demonstrating both strong and weak hydrogen bonding interactions in compound **I**.

and fragment patch, which offer pertinent proof of existing supramolecular interactions involved in the formation of molecular framework [25,26]. By mapping the molecular electrostatic potential using the computational tool TONTO, which is integrated with the CrystalExplorer programme, all Hirshfeld surfaces and fingerprint plots are produced [27]. Energy frameworks are generated using HF/3-21G basis sets for the cluster environment of 3.8 Å surrounding a particular molecule of interest. The total interaction energy is computed as $E_{tot} = k_{ele}E'_{ele} + k_{pol}E'_{pol} + k_{disp}E'_{disp} + k_{rep}E'_{rep}$, where the k values are scale factors for benchmark energy models, E'_{ele} is the electrostatic energy, E'_{pol} is the polarization energy, E'_{disp} is the dispersion energy, and E'_{rep} is the repulsive energy. The thickness of the cylinders produced during the calculation of the energy framework is directly correlated with the intensity of the interaction energies [5,28-30]. For compound **I**, the tube size is set by the factor of 100 with a cut-off energy of 5 kJ/mol to eliminate the crowdedness of insignificant interaction energies that are greater than van der Waals contacts.

3. Results and discussions

3.1. Crystal structure description

The Schiff's base **I** crystallizes in an orthorhombic crystal system with the $P2_12_12_1$ space group with one molecule of imine in the asymmetric unit. The molecule is puckered in shape with two aromatic rings lying out of the plane in a near anti-configuration across the C=N bond. The torsion angle across the imine bond is 169.65° involving atoms C7-N1-N2-C8. The molecule is stabilized by a number of noncovalent interactions with strong to moderately strong energies, which help the molecule to develop its complex supramolecular architecture in 3D. The diagram in Figure 2 shows the supramolecular framework of compound **I** where the molecules are interlocked with each other through strong and weak intermolecular hydrogen bonding contacts. The compound **I** bears weak intramolecular H10···N2 hydrogen bonding interaction with bond distance 2.626(2) Å and ∠C14-H10-N2 = 94.5°. The hydrogen atom H1 of -OH functionality of hydrazide entity forms bifurcated strong intermolecular hydrogen bonding interactions with N2 and O2 with bond distances H1···N2 and H1···O2 of 2.705(5) and 1.882(4) Å, respectively. The respective bond angles are ∠N2-H1-O1 = 129.84° and ∠O2-H1-O1 = 159.09°. The N-H hydrogen atom (H6) participates in strong intermolecular hydrogen bonding interaction with oxygen atom O1 of -OH functionality with bond distance H6···O1 of 2.135(8) Å and ∠N1-H6-O1 = 146.34° and interlocks the molecules into *a*-axis. The aromatic C-H (H2) involves in moderately strong C-H···π interaction with centroid of aromatic ring containing -OH functionality in a near edge-to-face fashion with bond distance H2···Cg1 = 2.588(11) Å and ∠Cg1-H2-C2 = 150.2°.

3.2. Hirshfeld surface and 2D fingerprint plots

The Hirshfeld surfaces are mapped over a d_{norm} ranging from -0.6660 to 1.0394 Å marking three different coloured regions on the surface: red regions representing stronger interactions with contacts less than van der Waals distance, blue regions portraying contacts more than van der Waals distance, and white regions manifesting inter-/intra-molecular contacts equal to van der Waals distance. The surface properties d_i and d_e are mapped in the ranges 0.6979 to 2.4193 Å and 0.6985 to 2.4970 Å, respectively. The other surface properties like shape index, surface curvedness, and fragment patch are plotted between -1 to 1, -4 to 0.4, and 0 to 15, respectively (Figure 3). The 2D fingerprint plots are generated by plotting d_e *vs.* d_i where surface coverages of various strong and weak noncovalent interactions are revealed quantitatively.

The d_{norm} surface is built over the surface volume 310.28 Å^3 and the surface area 311.84 Å^2, where the surface transparency allows a clear visualization of the molecule. The red regions on the surface mark the strong inter-/intra-molecular hydrogen bonding contacts present in the molecule while the white regions mark weaker contacts like Cl···O, Cl···Cl, Cl···H and Cl···N interactions. For the case of a strong hydrogen bonding interaction O···H, 14.3% of Hirshfeld surface coverage is observed revealing red regions on the d_{norm} surface and sharp spikes or tooth on 2D fingerprint plots (Figure 4).

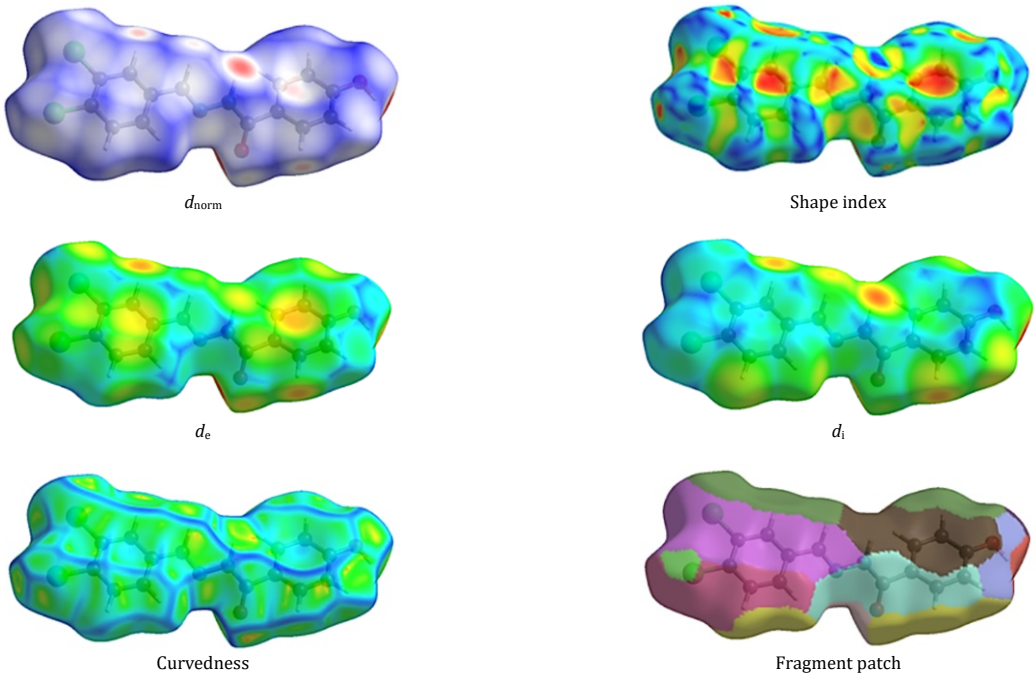

Figure 3. Hirshfeld surface analyses of compound **1**.

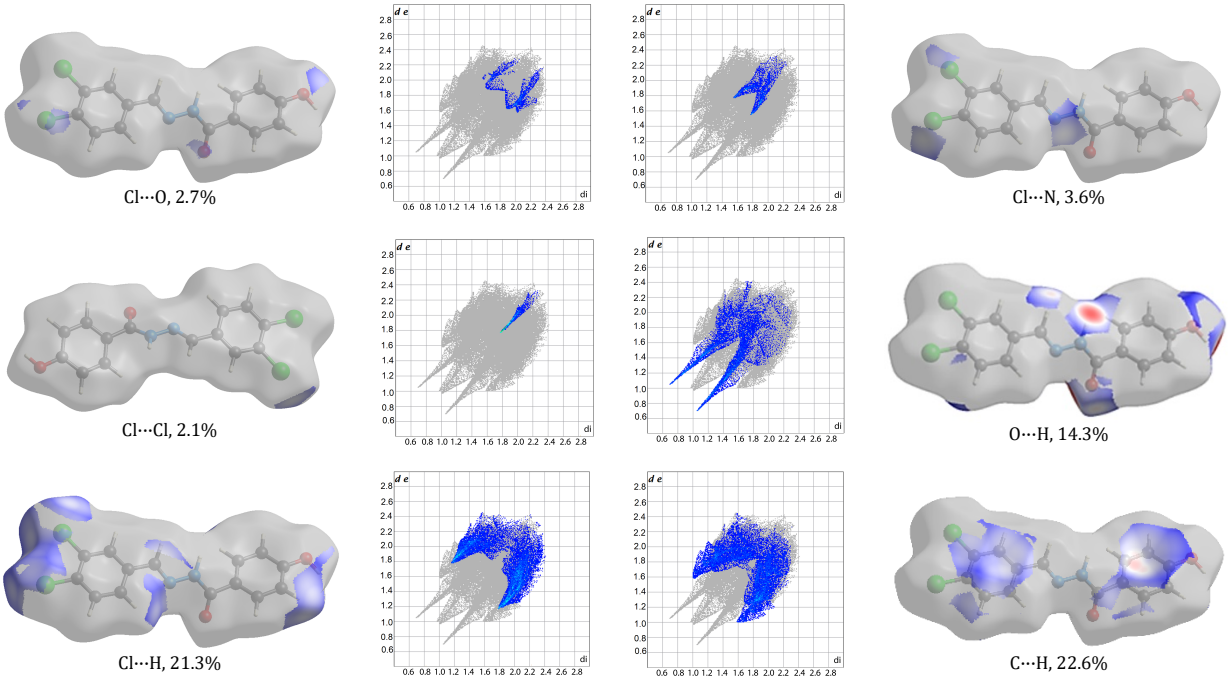

Figure 4. 2D fingerprint plots with mapped Hirshfeld surface contribution of supramolecular interactions involved in molecular packing of compound **I**.

Evidence of feeble Cl···Cl, Cl···O, and Cl···N weak interactions is observed on the d_{norm} surface with 2.1, 2.7, and 3.6% of the Hirshfeld surface coverage, respectively. The molecule is further stabilized by weak Cl···H and C···H hydrogen bonding contacts with 21.3 and 22.6% of Hirshfeld surface coverage. The d_{norm} surface exposures of all these weak interactions are shown in Figure 4. The shape indices and curvedness surface properties manifest further the varying energy dominated weak interactions in the molecular packing of crystal. The surface curvature is directly proportional to the strength of the interaction where lesser flat surface curvature specify that molecular packing is dominated by strong interactions like O-H···N/N-H···O hydrogen bonding interactions over other weaker interactions like π···π stacking, C-H···π, Cl···X (X = Cl, O, N) which contribute to lesser extent in packing of molecules in compound **I**. The red hollows in the shape index plot with index < 1 manifest a stronger interaction such as intermolecular/intramolecular hydrogen bonding. Other weaker interactions like Cl···O, Cl···Cl, Cl···H and Cl···N interactions along with weak Cl···H and C···H hydrogen bonding contacts demonstrate bumps in the shape index plot with index > 1.

Table 2. Interaction energy framework computation for compound **I** using HF/3-21G basis sets *.

Color	N	Symmetry operation	R	Electron density	E'_{ele}	E'_{pol}	E'_{disp}	E'_{rep}	E'_{tot}
	1	*x*, *y*, *z*	16.63	HF/3-21G	-4.9	-0.4	-3.2	0.0	-8.2
	0	*x*+1/2, -*y*+1/2, -*z*	11.32	HF/3-21G	-24.1	-8.2	-27.9	33.3	-28.0
	0	-*x*+1/2, -*y*, *z*+1/2	8.50	HF/3-21G	-62.1	-23.4	-52.9	77.2	-63.5
	1	*x*+1/2, -*y*+1/2, -*z*	6.61	HF/3-21G	-17.4	-5.1	-40.0	21.6	-39.6
	0	*x*, *y*, *z*	15.05	HF/3-21G	-2.2	-1.1	-8.1	0.0	-10.2
	0	-*x*, *y*+1/2, -*z*+1/2	6.66	HF/3-21G	-20.9	-7.5	-24.2	16.2	-34.9
	1	-*x*+1/2, -*y*, *z*+1/2	9.24	HF/3-21G	3.4	-1.6	-23.6	12.2	-8.9
	0	-*x*, *y*+1/2, -*z*+1/2	13.65	HF/3-21G	-3.5	-0.2	-4.5	0.0	-7.7

* Scale factors: k_{ele} = 1.019; k_{pol} = 0.651; k_{disp} = 0.901; k_{rep} = 0.811; Interaction energies (kJ/mol), R is the average distance between molecular centroids (Å), Total energies are obtained by multiplying individual energy contribution with computed scale factors and adding each component.

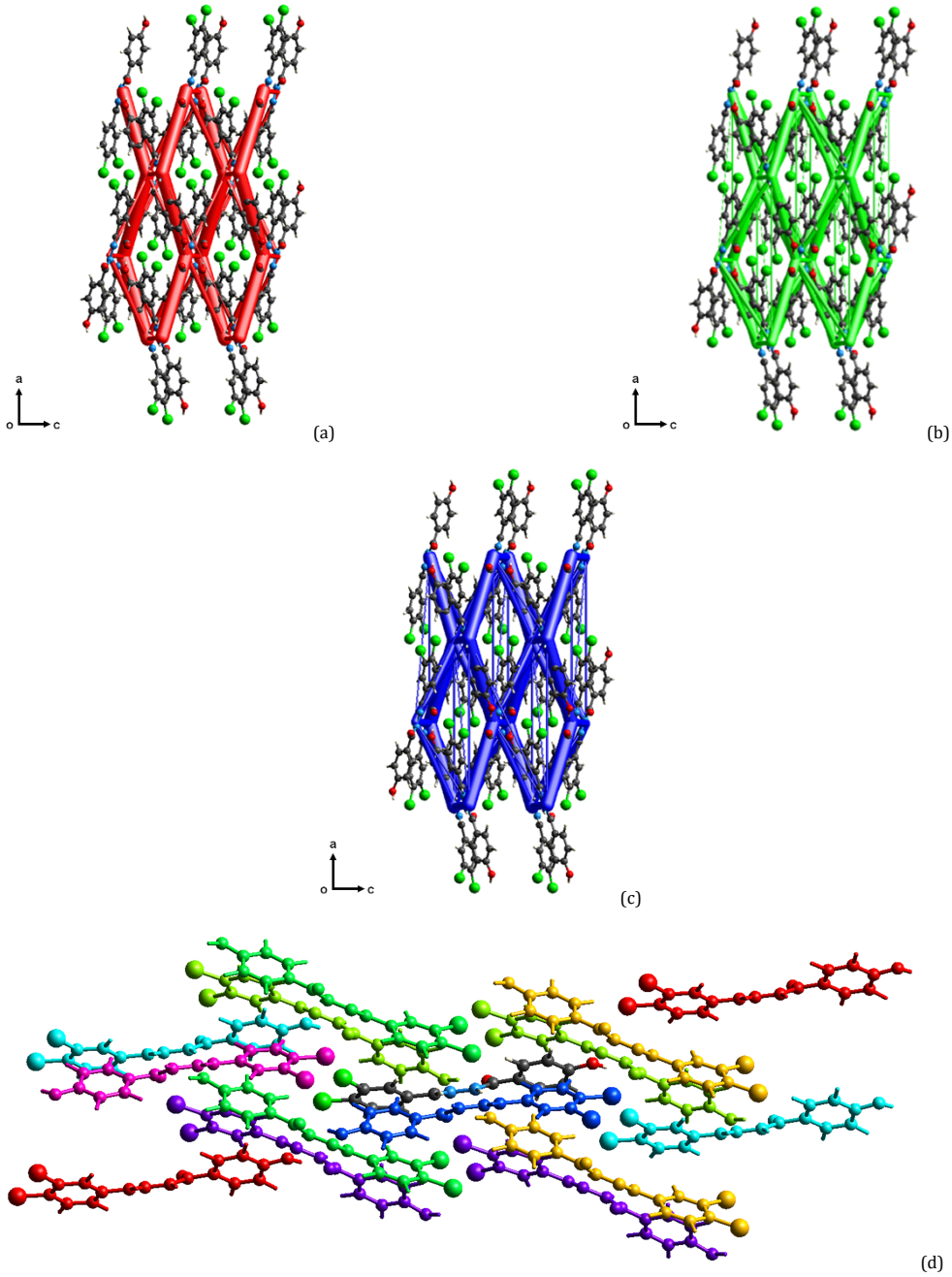

Figure 5. Representation of the Coulomb interaction energy (a), dispersion energy (b), total energy (c) in red, green, and blue colors, and molecular pairs involved in the calculation of interaction energies of compound **I** (d).

3.3. Interaction energy framework analysis

Energy framework analysis is crucial because a detailed understanding of the molecular topology of different intra-molecular/intermolecular interactions involved during the self-assembly of molecules in crystal packing through supra-molecular synthons [11]. Here, the interaction energies are determined by selecting a target molecule and developing a cluster environment of molecules at 3.8 Å distance by making use of the crystal lattice's symmetry operations; hence,

computing electronic, polarization, dispersive, and repulsive molecular wavefunctions, giving rise to total energies of the cluster.

Figure 5 demonstrates the energy framework analysis for compound **I** calculated using HF/3-21G electron densities with the highest stabilizing total interaction energy (-63.5 kJ/mol) obtained after the -*x*+1/2, -*y*, *z*+1/2 symmetry operation in molecules. Throughout the molecular framework, the least contribution in total energy, involved in stabilizing the crystal structure, is marked by the polarization energy, while electronic (Coulomb) and dispersive energies provide remarkable contributions in developing the supramolecular architecture of compound **I**. The nearly polar non-covalent interactions like strong hydrogen bonding comprise of electronic energy framework of the system while weaker and meagre interactions (other than hydrogen bonding) are addressed by dispersive nature. However, from 2D fingerprint plots we see that only 14.3% of Hirshfeld surface coverage (d_{norm}) is addressed by H···O interaction, while ~51% of Hirshfeld surface coverage (d_{norm}) is manifested through various weaker and dispersive interactions. Hence, dispersive interactions are the primary interactions that are involved in stabilizing the supramolecular framework of the crystal system of compound **I** (Table 2).

4. Conclusions

In conclusion, we have successfully demonstrated the synthesis of a new hydrazide functionalized Schiff's base complex (**I**) and have addressed its structural characterization with NMR spectroscopy, elemental analysis, and single crystal X-ray crystallography. Crystal structure analysis manifests near puckered orientation of aromatic rings across -C=N bond in an anti-configuration. Such a configuration can be the proof-of-concept behind the interlocked crystal packing in compound **I**. The structure-directing interactions involved in crystal packing are weak and dispersive in nature; electronic and dispersive energies provide notable contributions in developing supramolecular architecture as evident from energy framework analysis.

Acknowledgements

Archisman Dutta wishes to thank Geological Survey of India, Lucknow, for giving permission to pursue doctoral work at the Banaras Hindu University, India. Corresponding author acknowledges Prof. Biswajit Ray (Banaras Hindu University) for the constructive suggestions and rigorous review of the manuscript.

Supporting information

CCDC-2047308 contains the supplementary crystallographic data for this paper. These data can be obtained free of charge via www.ccdc.cam.ac.uk/data_request/cif, or by e-mailing data_request@ccdc.cam.ac.uk, or by contacting The Cambridge Crystallographic Data Centre, 12 Union Road, Cambridge CB2 1EZ, UK; fax: +44(0)1223-336033.

Disclosure statement

Conflict of interest: The authors declare that they have no conflict of interest.
Ethical approval: All ethical guidelines have been adhered.
Sample availability: Sample of the compound is available from the author.

CRediT authorship contribution statement

Conceptualization: Archisman Dutta; Methodology: Vivek Prakash Malviya, Archisman Dutta; Software: Archisman Dutta; Validation: Vivek Prakash Malviya, Archisman Dutta; Formal Analysis: Vivek Prakash Malviya, Archisman Dutta; Investigation: Vivek Prakash Malviya, Archisman Dutta; Resources: Vivek Prakash Malviya, Archisman Dutta; Data Curation: Vivek Prakash Malviya, Archisman Dutta; Writing - Original Draft: Vivek Prakash Malviya, Archisman Dutta; Writing - Review and Editing: Archisman Dutta; Visualization: Vivek Prakash Malviya, Archisman Dutta; Supervision: Archisman Dutta; Project Administration: Archisman Dutta.

ORCID and Email

Vivek Prakash Malviya
vivek.geology@gmail.com
https://orcid.org/0000-0001-6801-4087
Archisman Dutta
duttaarchisman1@gmail.com
archisman.dutta@gsi.gov.in
https://orcid.org/0000-0001-7142-8416

References

[1]. Desiraju, G. R.; Vittal, J. J.; Ramanan, A. *Crystal Engineering: A Textbook*; World Scientific Publishing: Singapore, Singapore, 2011.
[2]. He, J.; Wang, J.; Xu, Q.; Wu, X.; Dutta, A.; Kumar, A.; Muddassir, M.; Alowais, A.; Abduh, N. A. Y. Syntheses and crystal structures of new dinuclear lanthanide complexes based on 3-(4-hydroxyphenyl) propanoic acid: Hirshfeld surface analyses and photoluminescence sensing. *New J Chem* **2019**, *43*, 13499–13508.
[3]. Dutta, A.; Pan, Y.; Liu, J.-Q.; Kumar, A. Multicomponent isoreticular metal-organic frameworks: Principles, current status and challenges. *Coord. Chem. Rev.* **2021**, *445*, 214074.
[4]. Bauzá, A.; Seth, S. K.; Frontera, A. Tetrel bonding interactions at work: Impact on tin and lead coordination compounds. *Coord. Chem. Rev.* **2019**, *384*, 107–125.
[5]. Krishna, G. R.; Devarapalli, R.; Lal, G.; Reddy, C. M. Mechanically flexible organic crystals achieved by introducing weak interactions in structure: Supramolecular shape synthons. *J. Am. Chem. Soc.* **2016**, *138*, 13561–13567.
[6]. Desiraju, G. R. Supramolecular synthons in crystal engineering—A new organic synthesis. *Angew. Chem. Int. Ed. Engl.* **1995**, *34*, 2311–2327.
[7]. Diyali, N.; Chettri, M.; De, A.; Biswas, B. Synthesis, crystal structure, and antidiabetic property of hydrazine functionalized Schiff base: 1,2-Di(benzylidene)hydrazine. *Eur. J. Chem.* **2022**, *13*, 234–240.
[8]. Corey, E. J.; Cheng, X.-M. *The logic of chemical synthesis*; Wiley-Interscience: New York, 2009.
[9]. Dutta, A.; Mondal, S.; Singh, P. K.; Ray, B. Single crystal investigation, Hirshfeld surface and interaction energy framework analyses of structure-directing interactions within two isomorphous Schiff's base multicomponent salts. *J. Mol. Struct.* **2022**, *1264*, 133224.
[10]. Dutta, A.; Singh, A.; Wang, X.; Kumar, A.; Liu, J. Luminescent sensing of nitroaromatics by crystalline porous materials. *CrystEngComm* **2020**, *22*, 7736–7781.
[11]. Desiraju, G. R. Crystal engineering: From molecule to crystal. *J. Am. Chem. Soc.* **2013**, *135*, 9952–9967.
[12]. Saha, S.; Mishra, M. K.; Reddy, C. M.; Desiraju, G. R. From molecules to interactions to crystal engineering: Mechanical properties of organic solids. *Acc. Chem. Res.* **2018**, *51*, 2957–2967.
[13]. *Supramolecular assemblies based on electrostatic interactions*; Aboudzadeh, M. A.; Frontera, A., Eds.; 1st ed.; Springer International Publishing: Cham, Switzerland, 2022.
[14]. Mahmoudi, G.; Masoudiasl, A.; Babashkina, M. G.; Frontera, A.; Doert, T.; White, J. M.; Zangrando, E.; Zubkov, F. I.; Safin, D. A. On the importance of π-hole spodium bonding in tricoordinated HgII complexes. *Dalton Trans.* **2020**, *49*, 17547–17551.
[15]. Boldyreva, E. Mechanochemistry of inorganic and organic systems: what is similar, what is different? *Chem. Soc. Rev.* **2013**, *42*, 7719–7738.
[16]. Desiraju, G. R. Crystal engineering: A holistic view. *Angew. Chem. Int. Ed Engl.* **2007**, *46*, 8342–8356.
[17]. *Green approaches in medicinal chemistry for sustainable drug design*; Banik, B. K., Ed.; Elsevier Science Publishing: Philadelphia, PA, 2020.
[18]. Mahmoudi, G.; Abedi, M.; Lawrence, S. E.; Zangrando, E.; Babashkina, M. G.; Klein, A.; Frontera, A.; Safin, D. A. Tetrel bonding and other non-covalent interactions assisted supramolecular aggregation in a new Pb(II) complex of an isonicotinohydrazide. *Molecules* **2020**, *25*, 4056.
[19]. CrysAlisPRO, Oxford Diffraction /Agilent Technologies UK Ltd, Yarnton, England.
[20]. Dolomanov, O. V.; Bourhis, L. J.; Gildea, R. J.; Howard, J. A. K.; Puschmann, H. OLEX2: a complete structure solution, refinement and analysis program. *J. Appl. Crystallogr.* **2009**, *42*, 339–341.
[21]. Sheldrick, G. M. A short history of SHELX. *Acta Crystallogr. A* **2008**, *64*, 112–122.
[22]. Barbour, L. J. *X-Seed 4*: updates to a program for small-molecule supramolecular crystallography. *J. Appl. Crystallogr.* **2020**, *53*, 1141–1146.
[23]. Sheldrick, G. M. Crystal structure refinement with SHELXL. *Acta Crystallogr. C Struct. Chem.* **2015**, *71*, 3–8.
[24]. Spackman, M. A.; Jayatilaka, D. Hirshfeld surface analysis. *CrystEngComm* **2009**, *11*, 19–32.

[25]. Mackenzie, C. F.; Spackman, P. R.; Jayatilaka, D.; Spackman, M. A. CrystalExplorer model energies and energy frameworks: extension to metal coordination compounds, organic salts, solvates and open-shell systems. *IUCrJ* **2017**, *4*, 575–587.
[26]. Spackman, P. R.; Turner, M. J.; McKinnon, J. J.; Wolff, S. K.; Grimwood, D. J.; Jayatilaka, D.; Spackman, M. A. CrystalExplorer: a program for Hirshfeld surface analysis, visualization and quantitative analysis of molecular crystals. *J. Appl. Crystallogr.* **2021**, *54*, 1006–1011.
[27]. Jayatilaka, D.; Grimwood, D. J. Tonto: A FORTRAN based object-oriented system for quantum chemistry and crystallography. In *Lecture Notes in Computer Science*; Springer Berlin Heidelberg: Berlin, Heidelberg, 2003; pp. 142–151.
[28]. Frontera, A.; Bauzá, A. On the importance of σ–hole interactions in crystal structures. *Crystals (Basel)* **2021**, *11*, 1205.
[29]. Dutta, A.; Trivedi, M.; Alarifi, A.; Kumar, A.; Muddassir, M. A new 1D coordination polymer of triphenyl lead hydrosulfide: Synthesis and insights into crystal architecture and Hirshfeld surface analyses. *J. Mol. Struct.* **2020**, *1207*, 127801.
[30]. Yuan, F.; Zhang, R.; Qiao, C.-F.; Luo, X.-X.; Zhou, C.-S.; Wang, J.; Yang, Q.; Sakiyama, H.; Muddassir, M.; Dutta, A. Series of Ln-metal organic frameworks: Photocatalytic performance and Hirshfeld surface analyses. *J. Mol. Struct.* **2022**, *1251*, 131956.